71st International Astronautical Congress (IAC) – The CyberSpace Edition, 12-14 October 2020.

IAC-20,C3,4,3,x59509

A RESILIENCE APPROACH TO THE DESIGN OF FUTURE MOON BASE POWER SYSTEMS

Gianluca Filippi[a]*, Drew Gillespie [a], Andrew Ross Wilson [a], Massimiliano Vasile [a]

[a] *Department of Mechanical and Aerospace Engineering, University of Strathclyde, James Weir Building, 75 Montrose Street, Glasgow, G1 1XJ, United Kingdom*

* Corresponding Author: g.filippi@strath.ac.uk

Abstract

This paper proposes a novel approach to the design of complex engineering systems which maximise performance, and global system resilience. The approach is applied to the system level design of the power system for future Moon bases.

The power system is modelled as a network, where each node represents a specific power unit: energy storage, power distribution, power generation, power regulation. The performance and resilience of each power unit is defined by a mathematical model that depends on a set of design (control) and uncertain variables. The interrelationship among nodes is defined by functional links. The combination of multiple interconnected nodes defines the performance and resilience of the whole system.

An optimisation procedure is then used to find the optimal values of the design parameters. The optimal solution maximises global system resilience where an optimal resilient solution is either robust, i.e. it is not subject to disruptive failures, or recovers from failures to achieve a functioning state, albeit different from the starting one, after a contingency occurs.

The power system supports a Lunar base developed within the ESA-lab initiative, IGLUNA, led by the Swiss Space Centre. The power system, developed at the University of Strathclyde as part of the PowerHab project, is composed of nine interconnected elements: a hydrogen fuel cell energy storage system, a thermal mass storage system, a lithium-ion battery storage system, a constellation of solar power satellites (SPS) working in conjunction with a microwave wireless power transmission system, a reflecting satellite constellation and a ground-based solar power array. Distinct space and ground segments are identifiable, with orbit, AOCS and reflecting satellite nodes cooperating to provide optimal performance of the SPS constellation. The ground segment encompasses the ground-based solar array, energy storage systems, Lunar habitation module and the power transmission lines connecting these elements. Power generation is predominantly supplied by the ground-based array, with the SPS constellation and energy storage systems complementing this source; as well as providing redundancy and a reliable power supply during the Lunar night period.

Keywords: Resilience Optimization, Network, IGLUNA, Power System

Acronyms

ADCS Attitude Determination and Control System
AOCS Attitude and Orbit Control System
DC Direct Current
DOD Depth of Discharge
EPS Electrical Power System
ESA European Space Agency
GNC Guidance, Navigation and Control
HFC Hydrogen Fuel Cell
ISRU In-Situ Resource Utilisation
ISS International Space Station
ODE Ordinary Differential Equation
QoI Quantity of Interest
RFDN Radio Frequency Distribution Network
SA Solar Array
SBSP Space-Based Solar Power
SPS Solar Power Satellite
SRS Solar Reflector Satellite
TTC Tracking, Telemetry and Command System
UV Ultraviolet
WPT Wireless Power Transmission

1. Introduction

The next step for the space industry is to take humans back to the Moon. As stated in [1] and [2] the goal is to build a human habitat for possible long duration missions. Lunar surface exploration is indeed important for scientific purposes but also to demonstrate a technology's readiness for the next leap: the exploration of more distant planets. Both cases will require the realisation of all the infrastructures needed to guarantee survivability and an acceptable comfort for the permanence of astronauts. This paper is concerned with the study of a possible habitat on our Satellite and in particular with the design of a specific engineered

system: the electrical power system (EPS) for which a Space-based Solar Power (SBSP) concept is explored. The EPS needs to satisfy the power requirements of the whole settlement guaranteeing production, storage and distribution of electricity.

A general methodology for the design optimisation of complex engineered systems is presented. It is applied to the EPS, outlining its final optimal system architecture. The project will take a holistic view of the whole power supply where it is considered a complex system and it is optimised to be completely autonomous, reliable and resilient against critical scenarios, coming from huge uncertainty within the harsh and variable environment of the Moon's surface.

Uncertainty is taken into account by defining a set of mathematical models, one for each system's component, that depend on both decision (or design) and uncertain (or environmental) parameters. The network generated by the coupling of these models is finally optimised for resilience.

"Resilience engineering" is a new paradigm that has arisen in the research community in the last few years. As illustrated in [3], following the series of natural and man-made disasters that happened in the last 20 years, the presence of the word "resilience" and the associated "resilience approach" in engineering field increases exponentially in time in the scientific literature. Indeed, it is a common opinion that traditional approaches to deal with systems of increasing complexity cannot continue to be used. The necessity of this paradigm shift can be understood by analyzing the space shuttle Columbia accident [4]. The disruption was indeed certified to be caused by an inadequate organizational structure which was not able to circumvent the accident through anticipation, survive disruptions through recovery, and grow through adaptation. There was a fragmented problem solving that generated confusion at the system level and clouded the big picture. There were also problems of communication and cooperation between the different experts. As a consequence, production pressure eroded safety margins and exposed the system to the failure.

The term "resilience" can therefore be defined as the ability of the complex system to anticipate possible disruptions that could happen due to the involved uncertainty and to retain initial functionality after them. Finally, it is suggested that the proposed approach goes in the direction of solving the problems highlighted in [4] by creating a holistic view of the complex system by means of a network approach and by incorporating uncertainty in the optimization process and properly evaluating it.

1.1 Background

Overseen by the Swiss Space Center, the IGLUNA project is a collective of student teams, each tasked with developing solutions to enable a future ESA base on the Moon [5]. This paper derives from the work of the PowerHab project, the team fielded by the University of Strathclyde to develop a resilient solution to the issue of power generation, storage and distribution for the base.

2. Resilience Engineering

In the proposed optimization process two Quantities of Interest (QoIs) for the complex system, namely its performance M and its resilience measure R are defined by means of a mathematical model. The optimal design configuration is then found optimizing (minimizing) the performance M and satisfying the pre-defined requirements over the resilience R. The mathematical models takes into account the uncertainty affecting the complex system as they are function of both decision $\boldsymbol{d} \in D$ and uncertain $\boldsymbol{u} \in U$ variables: M(**d,u**) and R(**d,u**). In particular the QoIs are defined based on the topology of the network in which the complex system is translated:

$$\mathrm{M} = \sum_{j}^{N} M_i(\boldsymbol{d_i}, \overline{\boldsymbol{d}}_{\boldsymbol{i}}, \boldsymbol{u_i}, \overline{\boldsymbol{u}}_{\boldsymbol{i}}, \boldsymbol{\varphi_{ji}}) \qquad \text{Eq. 1}$$

$$\mathrm{R} = \sum_{j}^{N} R_i(\boldsymbol{d_i}, \overline{\boldsymbol{d}}_{\boldsymbol{i}}, \boldsymbol{u_i}, \overline{\boldsymbol{u}}_{\boldsymbol{i}}, \boldsymbol{\varphi_{ji}}) \qquad \text{Eq. 2}$$

In both Eq. 1 and Eq. 2, $\boldsymbol{d_i}$ and $\boldsymbol{u_i}$ are the vectors of design and uncertain parameters used only within the i-the node, $\overline{\boldsymbol{d}}_{\boldsymbol{i}}$ and $\overline{\boldsymbol{u}}_{\boldsymbol{i}}$ are vectors of components shared with other nodes and finally $\boldsymbol{\varphi_{ji}}$ is the set of coupling functions input in node i coming from nodes j where $\boldsymbol{\varphi_{ji}}(\boldsymbol{d_j}, \overline{\boldsymbol{d}}_{\boldsymbol{j}}, \boldsymbol{u_j}, \overline{\boldsymbol{u}}_{\boldsymbol{j}}, \boldsymbol{\varphi_{kj}})$.

The methodology then, can be formulated as the following constrained worst-case optimization:

$$\begin{cases} \min\limits_{d} \max\limits_{u} M \\ s.t. \ \min\limits_{u} R > \mu \end{cases} \qquad \text{Eq. 3}$$

This can be used to find the minimum of the function M over the design variables $\boldsymbol{d}$ considering its worst-case condition over the uncertain space U and that satisfy at the same time the requirement over R.

2.1 Global Resilience measure

Resilience is a dynamical measure related to the functionality of the system. Over the past years a strong understanding of the functional resilience of single components has been developed. Applying Bifurcation Theory to model the dynamics of the state x of an isolated system, the functional resilience can be expressed by an Ordinary Differential Equation (ODE) depending on x and β:

$$\frac{dx}{dt} = f(x, \beta) \qquad \text{Eq. 4}$$

where both x and β are functions of vectors **d** and **u** and the function f is problem specific. The bifurcation parameter β can lead to qualitative and topological shifts in the system dynamics even for small and smooth change of its value.

Engineered systems are however complex system consisting of a high number of connected components. For a generic system with N components, the couplings between sub-systems can be modelled by a network representation where each sub-system' state function x_i is considered:

$$\frac{dx_i}{dt} = f_i(x_i, \beta_i) + \sum_j^N a_{ij} g_i(x_i, \beta_i, x_j, \beta_j) \qquad \text{Eq. 5}$$

In Eq. 5 functions $f_i(.)$ and $g_i(.)$ model respectively the self-dynamics and the coupling dynamics while the components a_{ij} of the adjacency matrix A_{ij} define the topology of the network. The couplings are usually non-linear and they generate an emergent global dynamic of the whole system.

A measure for the global network system resilience can then be defined as:

$$\mathrm{R}(\mathbf{d}, \mathbf{u}) = \sum_j^N R_j = \sum_j^N \int_0^T x_j(t)\, dt \qquad \text{Eq. 6}$$

3. System Requirements

Staggered deployment is standard practice in the implementation of space systems. The clearest example of this was the construction of the International Space Station (ISS) which hosted multiple expeditions during the 13 years it took to fully assemble.

Previous studies have also taken this approach when defining the power requirements for lunar outpost concepts. Development is typically broken down into 3 to 5 phases [6, 7], however for simplicity these can be summarized as:

- Phase 1 – *Initial Development*
- Phase 2 – *Consolidation*
- Phase 3 – *Full-Scale Operations*

Power requirements differ between each study and deployment phase, however the consensus on initial development requirements are approximately 25kW,

with most work expected to be completed robotically [7, 8, 9, 10]. The consolidation phase varies greatly in the literature. However, it has most recently been defined by the International Space Exploration Coordination Group (ISECG) as "expansion and building" of a longer-term outpost [11]. Given this profile and the minimum threshold for outpost operations [10], the power requirement for this Phase 2 can be defined as 50kW. Phase 3 requirements are dependent on the objectives of the current mission, with the focus of this work being those outlined during the PowerHab project.

3.1 PowerHab Requirements and Constraints

Operation of the lunar base envisioned by the IGLUNA project is similar to that of the ISS, with a small number of additional systems specific to lunar habitation; such as rover exploration and in-situ resource utilization (ISRU).

Study of the ISS power system, and review of the total power budget for the other IGLUNA systems, led to a derived power requirement of 150kW; representing the 110kW capability of the ISS, with a 40% margin applied. This requirement for Phase 3 operations is given below in Table 1, alongside those for Phases 1 and 2 – which are outwith the scope of this paper.

Table 1: Power Requirements per Phase

Phase	***Description***	***Power Required*** *(kW)*
1	Initial Development	25
2	Consolidation	50
3	Full-Scale Operations	150

For the IGLUNA project, the location of the proposed base was constrained to the Shackleton Crater at the lunar south pole [12]. This location was chosen for the opportunity of ISRU of water ice; and some peaks of the crater remaining illuminated for up to 90% of the lunar year, thus minimizing power storage requirements [13].

4. System level Architectures

The analysed SBSP concept can be decomposed as in Figure 2 in a Space segment and in a Ground segment. The former includes a constellation of Solar Reflector Satellites (SRS) and a Solar Power Satellite (SPS). Each satellite consists of a payload - respectively the reflector and the Wireless Power Transmitter (WPT) - and a bus Figure 1 that combines all the other subsystems with the goal to support the payloads. The Ground segment is in charge of the generation (with SA and WPT receiver), storage (Batteries, Fuel Cells and Thermal Masses) and distribution of power.

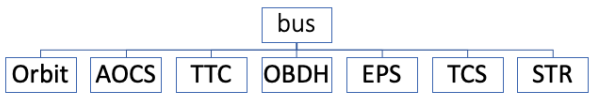

Figure 1: Spacecraft Bus decomposition

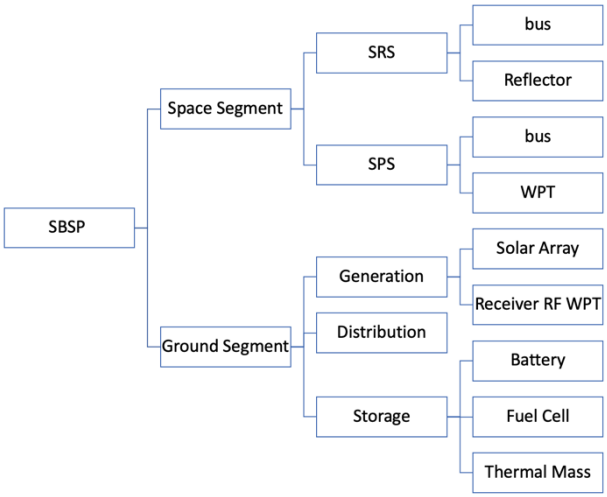

Figure 2: Block Diagram for the SBSP system

At the system level the following possible architectures have been modelled and considered in the design optimisation process. The space segment can be composed of either one (or more) SPS or a combination of SPS and SRS. The ground segment, instead, can involve any combination of Solar Array (SA), Battery, Hydrogen Fuel Cell (HFC) and Thermal Mass.

5. Sub-system level Architectures

Within each satellite one of the architectures summarized in Table 2 can be chosen. In case Solar Arrays (SAs) are used for the electrical power generation in conjunction with a Spin Stabilization AOCS, then the structural component of the power system is Body Mounted. In case a 3-axis stabilization AOCS is instead chosen, rigid panels are implemented and designed. For any other generation system (Secondary Batteries and Hydrogen Fuel Cells are considered within this paper) no specific model for the corresponding structural part has been considered.

Table 2: Sub-system Architectures

AOCS	***EPS***	***STR***
Spin stabilized	SA	Body mounted SA
3 axis	SA	Rigid panels SA
Any	Battery/HFC	No support for SA

6. Sub-system Models

This section provides a compact description of the mathematical models developed for the SBSP sub-systems. The interested reader can find more detailed analysis about the models for the spacecraft's bus in [14].

6.1 Orbit

A simple model has been implemented in the Orbit node. Indeed, 4 orbits have been found a-priori to be feasible for the SBSP system. They are reported in Table 3. Within the *mathematical* model then the eclipse period and the coverage period have been found by interpolation using the orbit parameters.

Table 3: Satellite coverage and eclipse

N	***a*** *(km)*	***Coverage*** *(h)*	***Eclipse*** *(h)*
1	1880	0.1	1.91
2	2250	0.45	2.25
3	6514	9.4	1.02
4	9250	22.17	1.33

6.2 Attitude and Orbit Control System

The Attitude and Orbit Control System (AOCS) includes two subsystems: Attitude Determination and Control System (ADCS) and Guidance, Navigation and Control System (GNC). The former's task is to stabilize the attitude of the satellite balancing external and internal disturbances in order to point payload (and possibly other subsystems) to its target with the required accuracy. The latter is instead involved in the maneuvers aiming to control and change orbit. For the present design analysis, the constellation of satellites already in its final orbit are considered, where focus will be placed upon the ADCS. As summarized in Table 2 two configurations are considered for the ADCS design. One is the spin stabilization. Here a number of thrusters allow the satellite to rotate around an inertial axis increasing its gyroscopic stiffness. The other option is given by the three-axis stabilization approach where the satellite maintains its orientation with respect to the nadir axis. In this case reaction wheels are used to balance solar, gravitational and magnetic disturbances while a choice between magneto-torques and thruster is used to unload them.

6.3 Telemetry and Telecommand System

The Telemetry and Tracking and Command System (TTC) is composed of a transmitter antenna, a receiver antenna, an amplified transponder and a radio frequency distribution network (RFDN). The TTC establish the telecommunication link between different satellites within the constellation and between each of them and the receiving antenna on the ground station. In particular a design parameter in the model can choose between patch, parabolic and horn antenna.

6.4 EPS

The functional breakdown of the EPS is in Figure 3 where the white rectangles represent the system decomposition while the shaded ones correspond to the design specialization. The EPS has indeed four main functions: to convert a source of energy into electric

power, to store a part of it in case it is not continuously available, to distribute electricity to all the spacecraft components and finally to regulate and control the generated power.

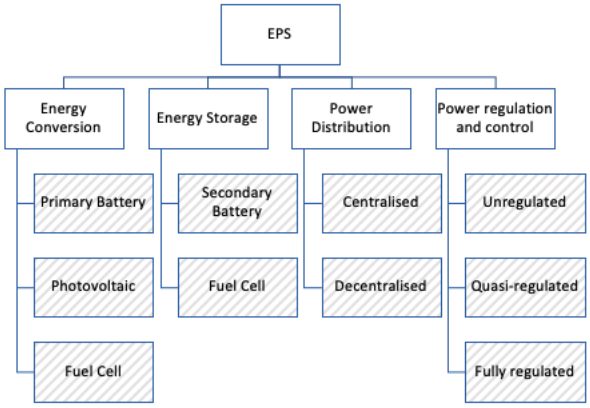

Figure 3: Electric Power Functional Decomposition

For the first function three options are here considered. Two of them, primary battery and fuel cell, convert electro-chemical energy and are analysed in the following sections while the photovoltaic option that converts solar radiation is describe here.

Table 4: Solar Cell Comparison

Cell	***Junction***	***Efficiency***	***Composition***
S-32	Single	17 %	Cz Si
3G28C	Triple	28%	GaInP/GaAs/ Ge
3G30C	Triple	30%	InGaP/GaAs/ Ge
4G32C	Quad	32%	AlInGaP/ AlInGaAs/ InGaAs/Ge

6.5 Structure

The Structure takes in consideration all the components that provide mechanical support to the other subsystems. Particular attention is paid to the EPS and in particular on the SA which has an important contribution for the overall system mass.

6.6 Solar Reflector

The solar reflector comprises a thin polymer membrane made of Aluminized-Mylar with a UV protective coating [15]. The membrane is stowed compactly before deployment in orbit. Expansion of the reflector from the stowed configuration is conducted using compressed nitrogen with inflatable beams, similar in design to the InflateSail [16] and L'Garde solar sail concepts [17].

The function of the solar reflector is to increase the solar irradiance, I, incident on the SPS solar array. The increased irradiance due to the reflection and concentration of the solar radiation, when operating in lunar orbit, is defined by:

$$I_f = \rho \frac{A_{SRS}}{A_f} cos\delta \cos\left(\frac{\theta}{2}\right) I \qquad \text{Eq. 7}$$

where the subscript f denotes parameters in the footprint region of the reflected radiation, ρ being the reflectance of the reflector membrane, δ the angle between the reflector normal and reflected beam and δ representing angle between the incident and reflected rays.

6.7 WPT Rectenna (Rx)

The ground-based rectifying antenna converts the incoming microwave beam from the SPS to DC electrical power. Consisting of a large array of microstrip patch antennae, sizing of the rectenna can be evaluated by:

$$P_r = \frac{P_{hab}}{\eta_{RFDC}} \qquad \text{Eq. 8}$$

$$A_r = \frac{P_r}{S_r} \qquad \text{Eq. 9}$$

where P_r and S_r denote the microwave power and average power density received respectively.

6.8 WPT Transmitter (Tx)

Review of the available literature on microwave WPT systems concludes an operating frequency of 94GHz for cislunar SBSP [18, 19]. Sizing of the transmitter could then be determined by Eq. 9 and Eq. *10* using the rectenna sizing and taking a suitable RF collection efficiency from comparable literature [18].

$$\eta_{RF} = 1 - e^{-\tau^2} \qquad \text{Eq. 10}$$

$$\tau = \frac{\sqrt{A_t A_r}}{\lambda d} \qquad \text{Eq. 11}$$

The electrical power required from the SPS to operate the transmitter can then be derived using:

$$P_{t_{in}} = \frac{P_r}{\eta_{RF} * \eta_{DCRF}} \qquad \text{Eq. 12}$$

Based on the microwave frequency and Phase 3 power requirement from Table 1, a gyrotron would be the

only oscillator capable of fulfilling this specification. A Cassegrain parabolic reflecting antenna is also incorporated into the transmitter design to improve the gain of the system.

6.9 Cables

Distribution of power in the ground segment occurs via transmission cables, similar to terrestrial power grids. Transmission cables considered for the lunar power system can be categorized by their voltage ratings outlined in Table 5.

Table 5: Transmission Cables Considered

Voltage Type	***Voltage Rating** (kV)*	***Purpose***
High	64.0 – 110.0	Primary Network Distribution
Medium	6.35 – 11.00	Connection from Primary Network to Sub-Grid
Low	0.60 – 1.00	Final Connection to Domestic Load

Careful consideration of the cable type applied is necessary as the different properties of each cable will affect the total mass and power losses of the cables; which are important in determination of the power requirements and mass of the overall system. These are evaluated by:

$$P_{loss} = I^2 Z \cos(\Phi)\, l \qquad \text{Eq. 13}$$

$$M_{cable} = ml \qquad \text{Eq. 14}$$

where m is in the form of mass per unit length.

6.10 Battery

The battery storage system is composed of a number of battery banks and battery management systems (BMS). Lithium-ion cells are arranged in modules inside of each bank, providing power during the lunar night and as a backup during system outages.

The critical equation in sizing the battery system is:

$$E_B = \frac{P_{req.} T_{ecl}}{\eta_{harn} DOD} \qquad \text{Eq. 15}$$

where the total energy required, E_B, is calculated using the habitat power requirement plus the power consumed by the BMS – which combined gives $P_{req.}$. The choice of cell is important as the cell specific energy is then used in determining the overall mass of the battery storage system.

6.11 Fuel Cell

The intended location of the base at the Shackleton Crater on the Moon presents an opportunity to employ ISRU for power storage and generation. Water ice, as discovered by *Chandrayaan-1* [20], can be melted and used in a regenerative HFC to store and generate energy. A regenerative HFC can convert hydrogen (H_2) and oxygen (O_2) gas to electrical energy and water; however, this can also be run in reverse to produce the gases from an input of water and electricity.

Sizing of the fuel cell and gas storage pressure vessels is dependent on the overall energy required, given by:

$$E_{req} = \frac{P_{req.} T_{ecl}}{\eta_{hfc}} \qquad \text{Eq. 16}$$

From Eq. 16 the volume of H_2 and O_2 gas required can be determined using the specific energy of hydrogen gas. Thus, the size and mass of the pressure vessels can be derived.

The power required for production of the gases from the electrolysis of water, can also be calculated from Eq. 17 and Eq. 18 below [21].

$$E = \frac{V_H \Delta G}{V_m} \qquad \text{Eq. 17}$$

$$P_e = \frac{E}{\eta_e t} \qquad \text{Eq. 18}$$

6.12 Thermal mass

Another application of ISRU, the thermal mass storage systems functions by concentration of solar radiation, using reflectors, to heat a working fluid which in turn heats a lump mass made of lunar regolith. A Stirling engine can then generate power, using the thermal mass as the high temperature reservoir, as required.

6.12.1 Stirling Engine

The coupling parameter used to size the system is the power of the Stirling engine, P_s. The efficiency of the Stirling engine is dictated by Eq. 19, where k_0 and τ represent the heat leak coefficient and cyclic period respectively. Heat transfer is described by Eq. 20, where χ substitutes a subscript 1 or 2, with the temperature of working fluid given by T_1 and T_2, at heat source T_H and sink T_L respectively; and effectiveness of the regenerator denoted by ε_R [22].

$$\eta_s = \frac{Q_1 - Q_2}{Q_1 + k_0 \tau (T_H - T_L)} \qquad \text{Eq. 19}$$

$$Q_{\chi} = nRT_{\chi} ln(\lambda) + c_v(1-\varepsilon_R)(T_1 - T_2) \quad \text{Eq. 20}$$

The mass and power of the Stirling engine can then be evaluated by:

$$P_s = \frac{P_{req.}}{\eta_s} \quad \text{Eq. 21}$$

$$M_s = \frac{P_s}{\dot{p}_s} \quad \text{Eq. 22}$$

where $\dot{p}_s$ is the specific power.

6.12.2 Fresnel Reflectors

The power of the Stirling engine can then be used in Eq. 23 to determine the area of Fresnel reflectors required, where η_o is the optical efficiency of the reflector, I is the incident solar radiation, C is the concentration ratio, h is the heat transfer coefficient, T_O is ambient temperature and ε the emissivity of the reflectors.

$$A_{FR} = \frac{P_s}{\left|\eta_o I - \frac{1}{C}\left[h(T_H - T_O) + \varepsilon\delta\left({T_H}^4 - {T_O}^4\right)\right]\right|} \quad \text{Eq. 23}$$

Thus, the overall mass of the reflector array can be calculated by Eq. 24, where ρ_{FR} is the areal density:

$$M_{FR} = A_{FR}\rho_{FR} \quad \text{Eq. 24}$$

7. Potential Failure Mechanisms

For each sub-system a failure tree analysis has been conducted and a reduced number of possible failure modes have been considered in the models. The loss of functionality x has been related to the design **d** and uncertain **u** vectors following Eq. *4* and Eq. *5*. In particular the trans-heteroclinic bifurcation [23] has been used.

8. Power System network

The optimization approach presented in Sec.2 is here applied to the design for resilience of the SBSP system for the human habitat on the Moon. Following Sec.6 and Sec.7 each sub-system model has been defined:

- model 1: Orbit
- model 2: TTC of the SRS
- model 3: AOCS of the SRS
- model 4: Thermal of the SRS
- model 5: Structure of the SRS
- model 6: Power of the SRS
- model 7: Reflector
- model 8: TTC of the SPS
- model 9: AOCS of the SPS
- model 10: Thermal of the SPS
- model 11: Structure of the SPS
- model 12: Power of the SPS
- model 13: WPT
- model 14: Ground Generation
- model 15: Ground Storage
- model 16: Ground Distribution

Table 6 and Table 7 collect their dimension with respect to the design space *D*, the uncertain space *U* and the number of directional links that couple the different subsystems.

Table 6: Space Segment model's dimension

Space Segment: SRS and SPS			
	dim d	*dim u*	*dim phi*
Orbit	5	1	0
AOCS	5	7	4
TTC	8	4	2
Thermal	9	4	2
Struct	2	0	1
Power	11	7	5
Reflector	5	2	0
WPT	4	0	2

Table 7: Ground Segment model's dimension

Ground Segment			
	dim d	*dim u*	*dim phi*
Generation	6	2	1
Storage	17	1	1
Distribution	5	3	0

The global performance measure *M* is here associated to the *Mass* and the global resilience measure R is constrained to be higher than 0.95. The optimization problem is then translated to:

$$\begin{cases} \min_{d} \max_{u} M \\ s.t. \ \min_{u} R > 0.95 \end{cases} \quad \text{Eq. 25}$$

9. Results

By combining the single node's models, the overall network can be defined, for which there are 88 design parameters and 31 uncertain parameters.

The couplings between subsystems are visualized in Figure 4, Figure 5, Figure 6 and Figure 7. In particular, Figure 4 shows all the couplings between nodes, Figure 5 only the directional links given by functions $\boldsymbol{\varphi_{ji}}$, Figure

6 only the non-directional links given by the sharing of design variables and Figure 7 the non-directional links given by shared uncertain parameters.

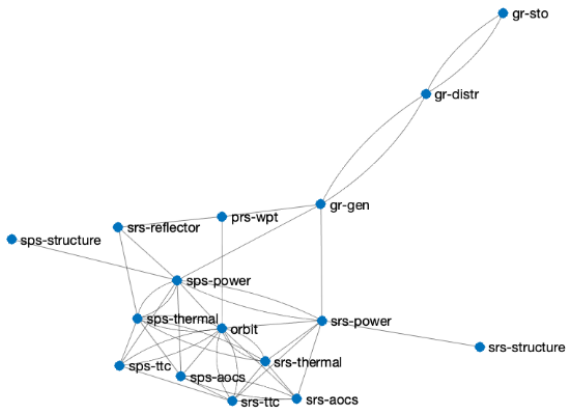

Figure 4: system network representation

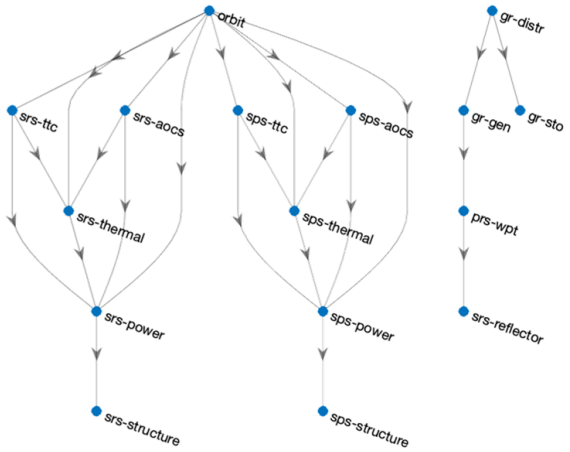

Figure 5: system network representation (only directional links)

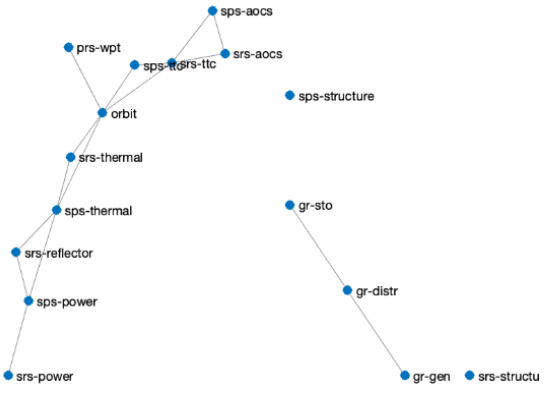

Figure 6: system network representation. Only non-directional links: sharing design variables

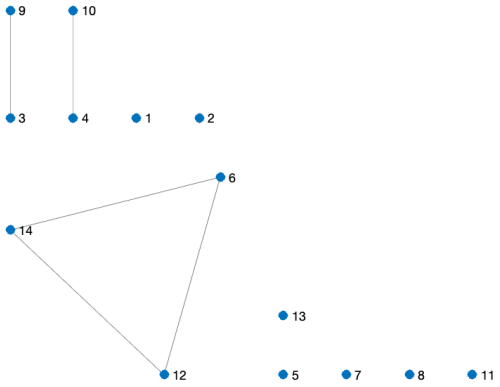

Figure 7: system network representation. Only non-directional links: sharing uncertain variables

The results of the optimisation for the overall network representing the complex engineered system (SBSP) are collected in Table 8. 'Mass 1' and 'Res 1' refer to the optimal solution for the unconstrained worst-case scenario where the resilience measure is not considered. 'Mass 2' and 'Res 2' are instead the optimal mass and resilience for the system where the constraint $\min_{\boldsymbol{u}} R \geq 0.95$ is used. Figure 8 finally compares the evolution in time of the global state x in Eq. 5 for the two optimal solutions.

As shown in Table 8 and Figure 8, by a modest increase in the final worst case total mass of the SBSP system, the optimisation process is able to find a solution satisfying the constraint on the global resilience. In particular, looking at Figure 8, the resilient solution (configuration 2 in Table 8) is able to sustain a shock and recover after it, while this is not possible for the non-resilient solution (configuration 1 in Table 8) where the measure R quickly converge to zero.

Table 8: Results

	Mass 1	***Mass 2***	***Res 1***	***Res 2***
SRS	137	146	0.0136	0.15
SPS	15438	18754	0.0102	0.27
Ground	140542	156329	0.0117	0.53
Tot	156117	175229	0.0355	0.95

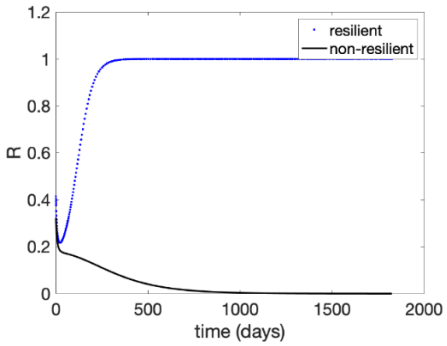

Figure 8: Resilience Results

10. Conclusions

This paper has introduced a new tool and a new approach for a model-based design of complex engineered systems that is based on an algorithmic optimisation for resilience. It has also applied the method in the design optimisation of the Space-based Solar Power System for a possible future human-based habitat on the Moon. The optimisation process starts by defining a mathematical model for each component of the complex system as function of design and uncertain parameters and by defining also the couplings between subsystems. The complex system is then automatically translated in a complex network where each node corresponds to a subsystem and the links are either directed couplings or sharing of design and/or uncertain variables between different nodes. Each mathematical model defines both the node's performance and its resilience measures where for the latter, the use of Bifurcation Theory is suggested. Finally, a worst-case optimisation procedure is implemented to optimise under uncertainty the corresponding global measures that arise from the nonlinear interactions between the network's nodes.

Acknowledgements

The authors would like to thank Samuel Beard, Donald Martin, Gareth Mitchell, Alex Potter, Gavin Rodgers, Finlay Rowe, Bradley Skelton and RS Components for their support and contributions to the IGLUNA 2020 project. This work was supported by the H2020-MSCA-ITN-2016 UTOPIAE, grant agreement 722734; and the Swiss Space Centre under the European Space Agency's ESA_Lab@CH initiative.

References

[1] M.A.Viscio, E.Gargioli, J.A.Hoffman, P.Maggiore, A.Messidoro and N.Viola, "A methodology to support strategic decisions in future human space exploration: From scenario definition to building blocks assessment," *Acta Astronautica*, pp. 198-217, 2013.

[2] M. A. Viscio, E.Gargioli, J. A. Hoffman, P. Maggiore, A. Messidoro and N. Viola, "A methodology for innovative technologies roadmaps assessment to support strategic decisions for future space exploration," *Acta Astronautica*, pp. 813-833, 2014.

[3] J. Park, T. P. Seager, P. S. Rao, M. Convertino and I. Linkov, Integrating risk and resilience approaches to catastrophe management in engineering systems, 2012.

[4] D. Woods, Creating foresight: How resilience engineering can transform NASA's approach to risky decision making, 2003.

[5] Swiss Space Centre, "IGLUNA," Swiss Space Centre, [Online]. Available: https://www.spacecenter.ch/igluna/. [Accessed 27 08 2020].

[6] Z. Khan, A. Vranis, A. Zavoico, S. Freid and B. Manners, "Power System Concepts for the Lunar Outpost: A Review of the Power Generation, Energy Storage, Power Management and Distribution (PMAD) System Requirements and Potential Technologies for Development of the Lunar Outpost," in *Space Technology and Applications International Forum*, Albuquerque, New Mexico, 2006.

[7] D. A. Petri, R. L. Cataldo and J. M. Bozek, "Power System Requirements and Definition For Lunar and Mars Outposts - A Review of the Space Exploration Initiative's NASA 90 Day Study," in *4th International Energy Conversion Engineering Conference and Exhibit*, San Diego, California, 2006.

[8] T. W. Kerslake, "Electric Power System Technology Options for Lunar Surface Missions," NASA, Cleveland, Ohio, 2005.

[9] B. H. Kenny and A. S. Coleman, "Power Management and Distribution Considerations for a Lunar Base," NASA, Cleveland, Ohio, 1992.

[10] NASA, "NASA Exploration Systems Architecture Study," NASA, 2005.

[11] International Space Exploration Coordination Group, "Global Exploration Roadmap," NASA, Washington, DC, 2020.

[12] R. Balasubramaniam, R. Wegeng, S. Gokoglu, N. Suzuki and K. Sacksteder, "Analysis of Solar-Heated Thermal Wadis to Support Extended-Duration Lunar Exploration," in *47th AIAA Aerospace Sciences Meeting including The New Horizons Forum and Aerospace Exposition*, Orlando, Florida, 2009.

[13] P.Gläser, F.Scholten, D. Rosa, R. Figuera, J.Oberst, E.Mazarico, G.A.Neumanne and S.Robinson, "Illumination conditions at the lunar south pole using high resolution Digital Terrain Models from LOLA," *Icarus*, vol. 243, pp. 78-90, 2014.

[14] G. Filippi, M. Vasile, D. Krpelik, P. Z. Korondi, M. Marchi and C. Poloni, "Space systems resilience optimisation under epistemic uncertainty," *Acta Astronautica*, vol. 165, pp. 195-210, 2019.

[15] N. Lior, "Mirrors in the sky: Status, sustainability, and some supporting," *Renewable and Sustainable Energy Reviews*, vol. 18, no. 1, pp. 401- 415, 2013.

[16] H. J. Kramer, "InflateSail," eoPortal, May 2019. [Online]. Available: https://directory.eoportal.org/web/eoportal/satellite-missions/i/inflatesail. [Accessed 10 november 2019].

[17] D. Lichodziejewski and B. Derbès, "Bringing an Effective Solar Sail Design Toward TRL 6," Huntsville, Alabama, 2003.

[18] M. M. Mojarradi, G. Chattopadhyay, H. Manohara, T. A. Vo, H. Mojaradi, S. Y. Bae and N. Marzwell, "Scalable Millimeter Wave Wireless Power Receiver Technology for Space Applications," in *AIAA SPACE 2008 Conference & Exposition*, San Diego, California, 2008.

[19] S. Mizojiri and K. Shimamura, "Wireless power transfer via Subterahertz-wave," *Applied Sciences*, vol. 8, no. 12, 2018.

[20] S. Li, P. G. Lucey, R. E. Milliken, P. O. Hayne, E. Fisher, J.-P. Williams, D. M. Hurley and R. C. Elphic, "Direct evidence of surface exposed water ice in the lunar polar regions," *Proceedings of the National Academy of Sciences*, vol. 115, no. 36, pp. 8907-8912, 2018.

[21] D. V. Schroeder, Introduction to Thermal Physics, Addison Wesley Longman, 1999.

[22] L. Yaqi, H. Yaling and W. Weiwei, "Optimization of solar-powered Stirling heat engine with finite-time thermodynamics," *Renewable Energy*, vol. 36, pp. 421-427, 2011.

[23] R. M. C. S. Josep Sardanyes, "Trans-heteroclinic bifurcation: a novel type of catastrophic shift," 2017.

[24] T. E. Bell, "Bizarre Lunar Orbits," 2006. [Online]. Available: https://science.nasa.gov/science-news/science-at-nasa/2006/06nov_loworbit/. [Accessed 31 March 2020].

[25] W. Reynolds, "Architecture Analysis of Wireless Power Transmission for Lunar Outposts," Monterey, California, 2015.

[26] P. E. Glaser, "Power from the Sun: Its Future," *Science*, vol. 162, pp. 857-861, 1968.

[27] C. Cougnet, E. S. (1), A. Celeste and L. Summerer, "SOLAR POWER SATELLITES FOR SPACE APPLICATIONS," in *55th International Astronautical Congress*, Vancouver, Canada, 2004.

[28] M. Arya, N. Lee and S. Pellegrino, "Ultralight Structures for Space Solar Power Satellites," in *3rd AIAA Spacecraft Structures Conference*, San Diego, California, 2016.

[29] Strategic Missions and Advanced Concepts Office, "Solar Power Technologies for Future Planetary Science Missions," NASA, Pasadena, California, 2017.

[30] J. C. Mankins and J. Howell, "Overview of the Space Solar Power Exploratory Research and Technology Program," in *35th Intersociety Energy Conversion Engineering Conference and Exhibit*, Las Vegas, Nevada, 2000.

[31] Z. Caineng, Z. Qun, Z. Guosheng and X. Bo, "Energy revolution: From a fossil energy era to a new energy," *Natural Gas Industry B*, vol. 3, no. 1, pp. 1-11, 2016.

[32] A. J. Peacock, "ABC of oxygen: Oxygen at high altitude," *British Medical Journal*, vol. 317, pp. 1063-1066, 1998.

[33] R. B.Malla and K. M.Brown, "Determination of temperature variation on lunar surface and subsurface for habitat analysis and design," *Acta Astronautica*, vol. 107, pp. 196-207, 2015.

[34] NASA, "Reference Guide to the International Space Station," NASA, Washington, DC, 2010.

[35] Boeing Mediaroom, "Boeing Ships LightSquared's SkyTerra 1 Mobile Communications Satellite to Launch Site," Boeing Defense, Space & Security, 19 October 2010. [Online]. Available: https://boeing.mediaroom.com/2010-10-19-Boeing-Ships-LightSquareds-SkyTerra-1-Mobile-Communications-Satellite-to-Launch-Site.

[36] J. Amos, "Huge antenna launched into space," BBC News, 2010.

[37] W. C. Brown, "RECTENNA TECHNOLOGY PROGRAM: Ultra Light 2.45 GHz Rectenna and 20 GHz Rectenna," NASA, Cleveland, Ohio, 1987.

[38] NASA, "Orion Quick Facts," 4 August 2014. [Online]. Available: https://www.nasa.gov/sites/default/files/fs-2014-08-004-jsc-orion_quickfacts-web.pdf.

[39] K. W. Billman, W. P. Gilbreath and S. W. Bowen, "Introductory assessment of orbiting reflections for terrestrial power generation," NASA United States, California, 1977.

[40] M. Yang and C. Zhou, "Comparison of different strategies to realize highly reflective thin film coatings at 1064 nm," *Infrared Physics & Technology*, vol. 51, no. 6, pp. 572-575, 2008.

[41] L. Barron, "High-reflectance, sputter-deposited aluminum alloy thin thin films for micro-electro-mechanical systems," Rochester Institute of Technology, Rochester, 2005.

[42] R. Pappa, G. Rose, T. Mann, J. Warren, M. Mikulas, T. Kerslake, T. Kraft and J. Banik, "Solar Array Structures for 300 kW-Class Spacecraft," in *Space Power Workshop*, Manhatten Beach, California, 2013.

[43] M. F. Ashby, Materials and the Environment: Eco-Informed Material Choice, Oxford: Butterworth-Heinemann, 2013.

[44] J. R. Wertz, D. F. Everett and J. J. Puschell, Space Mission Engineering: The New SMAD, Hawthorne, California: Microcosm Press, 2015.

[45] M. Ashby, "Material property data for engineering materials," Granta Design, Cambridge, UK, 2016.

[46] AZUR SPACE Solar Power GmbH, "SPACE Solar Cells," AZUR SPACE Solar Power GmbH, 2019. [Online]. Available: http://www.azurspace.com/index.php/en/products/products-space/space-solar-cells.

[47] H.-K. Chiou and I.-S. Chen, "High-Efficiency Dual-Band On-Chip Rectenna for 35- and 94-GHz Wireless Power Transmission in 0.13-□m CMOS Technology," *IEEE TRANSACTIONS ON MICROWAVE THEORY AND TECHNIQUES*, vol. 58, no. 12, 2010.

[48] T.-W. Yoo and K. Chang, "Theoretical and Experimental Development of 10 and 35 GHz Rectennas," *IEEE TRANSACTIONS ON MICROWAVE THEORY AND TECHNIQUES*, vol. 40, no. 6, 1992.

[49] Z.-Q. Liu, H. Qiu, X. Li and S.-L. Yang, "Review of Large Spacecraft Deployable Membrane Antenna Structures," *Chinese Journal of Mechanical Engineering*, vol. 30, pp. 1447-1459, 2017.

[50] R. C. Hansen, "32 - Antennas," in *Reference Data for Engineers: Radio, Electronics, Computer, and Communications (Ninth Edition)*, Newnes, 2002, pp. 1-58.

[51] A. Kasugai, K. Sakamoto, K. Takahashi, K. Kajiwara and N. Kobayashi, "Steady-state operation of 170 GHz–1 MW," *Nuclear Fusion*, vol. 48, 2008.

[52] D. Borodin, R. Ben-Moshe and M. Einat, "Design of 95 GHz gyrotron based on continuous operation copper solenoid with water cooling," *Review of Scientific Instruments*, vol. 85, 2014.

[53] Canon Electron Tubes & Devices, "Microwave Tubes / Power Grid Tubes - Gyrotrons," Canon Electron Tubes & Devices, 2020. [Online]. Available: https://etd.canon/en/product/category/microwave/gyrotron.html.

[54] C. Lei, S. Yu, H. Li, Y. Liu and Q. Zhao, "Design and numerical simulation of a 94 GHz gyrotron with gradually tapered cavity," *Qiangjiguang Yu Lizishu/High Power Laser and Particle Beams*, vol. 26, no. 2, 2014.

[55] J. M. Neilson, M. Read and R. L. Ives, "P3-4: Design and assembly of a permanent magnet gyrotron for active denial systems," in *IEEE International Vacuum Electronics Conference* , Monterey, California, 2010.

[56] "Beamed Microwave Power Transmission and its Application to Space," *IEEE TRANSACTIONS ON MICROWAVE THEORY AND TECHNIQUES*, vol. 40, no. 6, 1992.

[57] K. Minakawa, K. Matsui, W. Komurasaki, Y. Hatakeyama, O. K., M. Suzuki, K. Shimamura, A. Mizushima, K. Fujiwara and H. Yamaoka, "Microstrip antenna and rectifier for wireless power transfar at 94GHz," in *IEEE Wireless Power Transfer Conference*, Taipei, Taiwan, 2017.

[58] S. C. Aleina, N. Viola, R. Fusaro and G. Saccoccia, "Approach to technology prioritisation in support of Moon initiatives in the framework of ESA exploration technology roadmaps," 2017.